

Neural stem cell-conditioned medium ameliorates $A\beta_{25-35}$ -induced damage in SH-SY5Y cells by protecting mitochondrial function

Guoyong Jia, Zengyan Diao, Ying Liu, Congcong Sun, Cuilan Wang*

ABSTRACT

Inhibition of amyloid β ($A\beta$)-induced mitochondrial damage is considered crucial for reducing the pathological damage in Alzheimer's disease (AD). We evaluated the effect of neural stem cell-conditioned medium (NSC-CDM) on $A\beta_{25-35}$ -induced damage in SH-SY5Y cells. An *in vitro* model of AD was established by treating SH-SY5Y cells with 40 μ M $A\beta_{25-35}$ for 24 h. SH-SY5Y cells were divided into control, $A\beta_{25-35}$ (40 μ M), $A\beta_{25-35}$ (40 μ M) + NSC-CDM, and $A\beta_{25-35}$ (40 μ M) + neural stem cell-complete medium (NSC-CPM) groups. Cell viability was detected by CCK-8 assay. Apoptosis, reactive oxygen species (ROS) production, and mitochondrial membrane potential (MMP) were detected by flow cytometry. Malondialdehyde content was detected by ELISA assay. Western blot analysis was used to detect cytochrome c release and apoptosis-related proteins. Transmission electron microscopy was used to observe mitochondrial morphology. Cell viability significantly decreased and apoptosis significantly increased in SH-SY5Y cells treated with $A\beta_{25-35}$, and both effects were rescued by NSC-CDM. In addition, NSC-CDM reduced ROS production and significantly inhibited the reduction of MMP caused by $A\beta_{25-35}$. Furthermore, NSC-CDM ameliorated $A\beta_{25-35}$ -induced reduction in Bcl-2 expression levels and increased the expression levels of cytochrome c, caspase-9, caspase-3, and Bax. Moreover, $A\beta_{25-35}$ induced the destruction of mitochondrial ultrastructure and this effect was reversed by NSC-CDM. Collectively, our findings demonstrated the protective effect of NSC-CDM against $A\beta_{25-35}$ -induced SH-SY5Y cell damage and clarified the mechanism of action of $A\beta_{25-35}$ in terms of mitochondrial maintenance and mitochondria-associated apoptosis signaling pathways, thus providing a theoretical basis for the development of novel anti-AD treatments.

KEYWORDS: Alzheimer's disease; neural stem cell-conditioned medium; $A\beta_{25-35}$; mitochondria; apoptosis

INTRODUCTION

Alzheimer's disease (AD) is the most common neurodegenerative disease. Recently, AD has attracted increasing attention for its social harm and high incidence in the elderly population [1]. With the global aging of the population, the development of prevention strategies and effective treatments for AD is considered extremely urgent. The pathogenesis of AD is complex, with the development of senile plaques and neurofibrillary tangles formed by β -amyloid (amyloid β , $A\beta$) deposition considered hallmark features [2]. Studies have shown that $A\beta$ can directly or indirectly damage the structure and function of mitochondria, resulting in the induction of oxidative stress and the activation of the

apoptotic signaling pathway cascade [3]. Moreover, these processes in themselves serve to promote $A\beta$ production, further aggravating mitochondrial damage and resulting in a vicious cycle, leading to neuronal degeneration and apoptosis. Therefore, inhibition of $A\beta$ -induced mitochondrial damage is considered crucial for reducing the pathological damage in AD [4].

Neural stem cells (NSCs) are a type of stem cell with self-renewal and neural differentiation capability. NSCs are abundant in the subventricular zone of adults and the subgranular layer of the hippocampal dentate gyrus [5], which serves as a stem cell pool for biologically replacing damaged nerve tissue. The unique neurorestorative capacity of the hippocampal dentate gyrus makes NSC transplantation the most promising treatment for a variety of neurological diseases, including Parkinson's disease and AD [6]. To date, NSC transplantation methods have achieved good therapeutic effects in basic experiments. However, the isolation of NSCs is difficult and ethical issues exist surrounding their use. In addition, exogenous cell transplantation often adversely affects the growth of the transplanted cells due to host immune rejection and damage to the pathological microenvironment [7]. Therefore, the clinical use of NSCs in transplantation procedures faces a number of obstacles [8]. Considering that

Department of Neurology, Qilu Hospital, Shandong University, Jinan, China

*Corresponding author: Cuilan Wang, Department of Neurology, Qilu Hospital, Shandong University, No. 107 West Wenhua Road, Jinan, Shandong 250012, China. E-mail: qlyywcl1961@163.com

DOI: <https://dx.doi.org/10.17305/bjbms.2020.4570>

Submitted: 17 December 2019/Accepted: 23 February 2020

Conflict of interest statement: The authors declare no conflict of interests



©The Author(s) (2021). This work is licensed under a Creative Commons Attribution 4.0 International License

the repair mechanism of NSC transplantation involves the replacement of the original neural tissue, there are additional requirements to consider, including immune conditioning and neurotrophic support produced by associated paracrine products [9]. Studies have shown that NSC-conditioned medium (NSC-CDM) can increase the *in vitro* expression of M2 macrophages, reduce M1 type activation, and inhibit the release of multiple inflammatory factors [10]. Similarly, *in vivo* experiments have shown that the injection of NSC-CDM into rats with spinal cord injury increases the bridging needed between the corticospinal tract and interneurons, thus reducing neuronal apoptosis and promoting motor function recovery [11]. Therefore, the use of NSC-CDM to replace the original secretions of these cells has become a new therapeutic strategy that can effectively avoid a number of problems, including ethics issues, transplant cell survival, cell preservation, and transportation.

In this study, our findings demonstrated that NSC-CDM is protective against A β_{25-35} -induced cytotoxicity, including apoptosis, reduced cell viability, and damage to the mitochondrial ultrastructure, in SH-SY5Y cells. In addition, further analysis of mitochondrial apoptosis-related proteins indicated that the protective effect of NSC-CDM is due to the modulation of the intrinsic apoptotic pathway.

MATERIALS AND METHODS

A β_{25-35} preparation

Five milligrams of A β_{25-35} (Sigma-Aldrich, St. Louis, MO, USA) was dissolved in 5 mL double-distilled water. A micron microporous filter (0.22 μ m) was sterilized by filtration under sterile conditions and placed in a 37°C incubator for 7 days. A small sample was taken for protein concentration determination and stored at -20°C for later use.

Cell culture and treatment

Logarithmic growth phase human SH-SY5Y cells (N7800-100, Thermo Fisher Scientific, USA) were collected, counted, and resuspended in Dulbecco's Modified Eagle Medium/Ham's F-12 (DMEM/F-12) complete medium [CPM] (11320033, Gibco, USA) containing 10% fetal bovine serum [FBS] (10099133, Gibco) and 1% double antibody. The cell concentration was adjusted to 1×10^5 cells/mL and the cells were seeded in 6-well plates, with 2 mL of cell suspension per well. The plates were incubated at 37°C overnight at 5% CO₂. After the cells were fully attached, the medium in the wells was discarded and the plates were prepared according to the experimental group. For the control group, 2 mL of DMEM/F-12 medium containing 10% FBS was added to the 6-well plate. For the A β_{25-35} group, A β_{25-35} and DMEM/F-12 medium

containing 10% FBS were added to the 6-well plate, with the final concentration of A β_{25-35} 40 μ M. For the A β_{25-35} + NSC-CDM group, A β_{25-35} and 10% FBS containing NSC-CDM were added to the 6-well plate, with the final concentration of A β_{25-35} 40 μ M. For the A β_{25-35} + NSC-CPM group, A β_{25-35} and 10% FBS containing NSC-CPM were added to the 6-well plate, with the final concentration of A β_{25-35} 40 μ M. The isolation and culturing of the NSCs and the NSC-CDM were performed according to our previous study [12].

CCK-8 analysis

SH-SY5Y cells were grown at $2-4 \times 10^4$ cells/well in 96-well microplates. The CCK-8 solution (CK04, Sigma-Aldrich, USA) was then added to the medium to a final concentration of 0.5 mg/mL and incubated for 4 h at 37°C. The absorbance was read at 450 nm by Multiskan FC (Thermo Scientific, USA) and the cell viability was determined.

Apoptosis analysis

Using an *in situ* cell death detection kit (Roche, Mannheim, Germany), the cells were grown on coverslips, followed by the terminal deoxynucleotidyl transferase-mediated dUTP nick end labeling (TUNEL) assay. After TUNEL labeling, the sections were observed using a light microscope (Olympus, Tokyo, Japan) to detect apoptotic cells at $\times 400$ magnification, with a view size area of 0.344 mm². The cells that were positively stained with the TUNEL stain presented as a dark red color under the light microscope and were considered to be apoptotic.

Flow cytometry analysis

The Annexin V-FITC/PI Apoptosis Detection Kit (Becton Dickinson, Rutherford, NJ, USA) was used for the quantification of cellular apoptosis. Briefly, the cells were resuspended in 200 μ L annexin binding buffer containing 5 μ L PI and 10 μ L annexin V-FITC in the dark for 10 min at 25°C. Flow cytometry (Abcam, USA) was used to analyze the double-stained cells.

Assessment of reactive oxygen species (ROS) production

Mitochondrial ROS production was evaluated using specific ROS kits (GenMed Scientifics Inc., Wilmington, DE). Mitochondrial fractions (50 μ g) were cultured with 6-chloromethyl-2',7'-dichlorodihydro-fluorescein diacetate (CM-H₂DCFDA) at 37°C for 15 min. Fluorescence, with excitation and emission wavelengths of 490 and 530 nm, respectively, was monitored by a fluorescence spectrophotometer.

Determination of malondialdehyde (MDA) activity

SH-SY5Y cells were centrifuged for 15 min at 4500 rpm. The samples were stored at -80°C prior to the analysis of MDA activity, which was evaluated using a commercial ELISA kit (A003-4-4, Nanjing Built Bio, Nanjing, China).

Transmission electron microscopy (TEM)

SH-SY5Y cells at 5×10^6 cells/mL were incubated in Schneider medium at 25°C for 24 h. After washing with phosphate-buffered saline (PBS), the cells were fixed in 2.5% glutaraldehyde in 0.1 M sodium cacodylate buffer (pH 7.2) at 25°C for 40 min and post-fixed in a solution containing 1% osmium tetroxide, 0.8% potassium ferricyanide, and 2.5 mM CaCl_2 for 20 min. The cells were then dehydrated with acetone and embedded in PolyBed 812 resin. Ultrathin sections ($0.06 \mu\text{m}$) were sliced and stained with uranyl acetate and lead citrate, followed by examination with a JEM-1200 EX electron microscope by a blinded examiner.

Determination of mitochondrial membrane potential (MMP)

MMP was evaluated using a specific MMP kit (Beyotime, Haimen, China) that included JC-1 (5,5',6,6'-tetrachloro-1,1',3,3'-tetraethyl-imida carbocyanine iodide, C2006, Biyuntian, Shanghai, China), which is a fluorochrome that becomes incorporated into cells depending on the status of the MMP. In this process, staining for reduced JC-1, which emits green fluorescence, indicates a disruption of the mitochondrial inner-membrane potential. Briefly, SH-SY5Y cells in 6-well plates were processed as described in previous experiments, washed with PBS, and cultured with the JC-1 solution at 37°C for 20 min in the dark. The cells were then washed twice with PBS and resuspended in PBS ($500 \mu\text{L}$). Fluorescence was evaluated by a BD FACSAria II flow cytometer system (BD, Franklin Lakes, NJ). The results are shown in terms of the proportion of cells with a low MMP.

Western blot analysis

Proteins were examined via Western blot analysis using monoclonal antibodies against the cytochrome c (1:1000, Ab13575, Abcam, USA), caspase-9 (1:1000, Ab52298, Abcam), caspase-3 (1:500, Ab2302, Abcam), Bcl-2-associated X protein [Bax] (1:2000, Ab32503, Abcam), and B-cell lymphoma 2 [Bcl-2] (1:500, Ab32124, Abcam, USA) proteins. β -actin (1:5000, Sigma, USA) served as the loading control. A horseradish peroxidase (HRP)-labeled secondary antibody (1:1000, Santa Cruz, USA) was used and cultured with the cells for 1 h at 25°C . Quantification of the band density was performed using

a LI-COR Odyssey infrared imaging system (LI-COR Bioscience, Nebraska, USA).

Statistical analysis

The GraphPad Prism version 8.00 for Windows (GraphPad Software, La Jolla California USA) was used to analyze the data. All experiments were repeated 3 times and the mean \pm standard deviation was used for all analyses. ANOVA was used to determine whether marked differences existed among the experimental groups, with $p < 0.05$ regarded as significant.

RESULTS

A β_{25-35} -induced damage in SH-SY5Y cells

A β_{25-35} ($40 \mu\text{M}$) was used to treat the SH-SY5Y cells for different time periods and the cell survival rate was shown to decrease with time. When the time was increased to 36 h, the cell viability decreased to $58.62 \pm 1.26\%$ compared with the control group ($p < 0.05$; Figure 1A). Different concentrations of A β_{25-35} were then used to treat the SH-SY5Y cells for 24 h. As the concentration of A β_{25-35} increased, the cell survival rate decreased gradually. At $40 \mu\text{M}$, the cell viability decreased to $56.62 \pm 1.26\%$ compared with the control group ($p < 0.05$; Figure 1B).

NSC-CDM rescued A β_{25-35} -induced cytotoxicity, including decreased cell viability and increased apoptosis, in SH-SY5Y cells

To investigate the effects of NSC-CDM in SH-SY5Y cells, the cell viability of the cells was evaluated by CCK-8 assay in the control, A β_{25-35} ($40 \mu\text{M}$), A β_{25-35} ($40 \mu\text{M}$) + NSC-CPM, and A β_{25-35} ($40 \mu\text{M}$) + NSC-CDM groups for 24 h. As shown in Figure 2A, A β_{25-35} significantly decreased the cell viability of the SH-SY5Y cells as compared with the control group ($p < 0.001$). In contrast, both NSC-CPM and NSC-CDM had an inhibitory effect on the cytotoxicity induced by A β_{25-35} ($p < 0.001$ and $p < 0.01$, respectively), with the NSC-CDM group demonstrating a higher cell viability than the NSC-CPM group ($p < 0.05$). Next, we applied TUNEL and annexin V-FITC/PI double-staining to determine the number of apoptotic SH-SY5Y cells. As demonstrated in Figure 2B and C, the nuclear fragmentation that is a characteristic feature of apoptotic cells was clearly observed in the A β_{25-35} -induced SH-SY5Y cells. In addition, condensed nuclei were also identified. However, the numbers of TUNEL-positive nuclei were significantly lower in the NSC-CPM or NSC-CDM + A β_{25-35} -treated cells, with the NSC-CDM group demonstrating a lower number of TUNEL-positive nuclei than the NSC-CPM group. In addition, cellular apoptosis was examined by annexin V-FITC/PI double-staining and showed the same trends (Figure 2D).

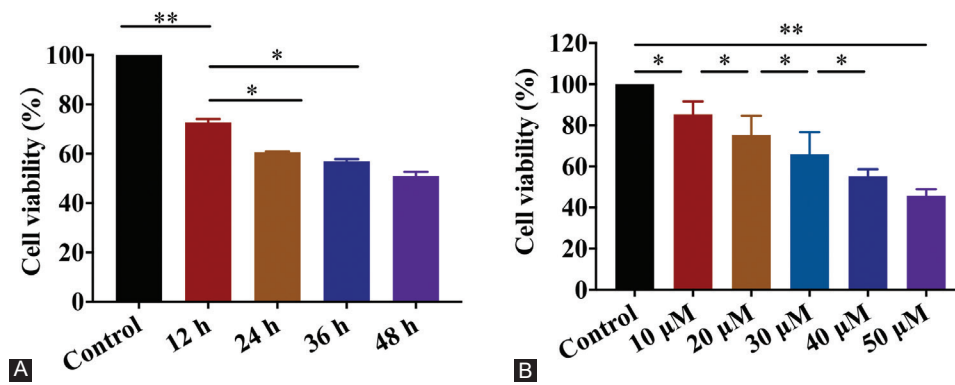


FIGURE 1. Different concentration and time of $A\beta_{25-35}$ treatment in SH-SY5Y cells. (A) CCK-8 detection of $A\beta_{25-35}$ (30 μM) treatment in SH-SY5Y cells for 12, 24, 36, and 48 h. (B) CCK-8 detection of $A\beta_{25-35}$ (0, 10, 20, 30, 40, and 50 μM) treatment in SH-SY5Y cells for 24 h. * $p < 0.05$, ** $p < 0.01$. When the time was increased to 36 h, the cell viability decreased to $58.62 \pm 1.26\%$ compared with the control group. Different concentrations of $A\beta_{25-35}$ were then used to treat SH-SY5Y cells for 24 h. As the concentration of $A\beta_{25-35}$ increased, the cell survival rate decreased gradually. At 40 μM , the cell viability decreased to $56.62 \pm 1.26\%$ compared with the control group.

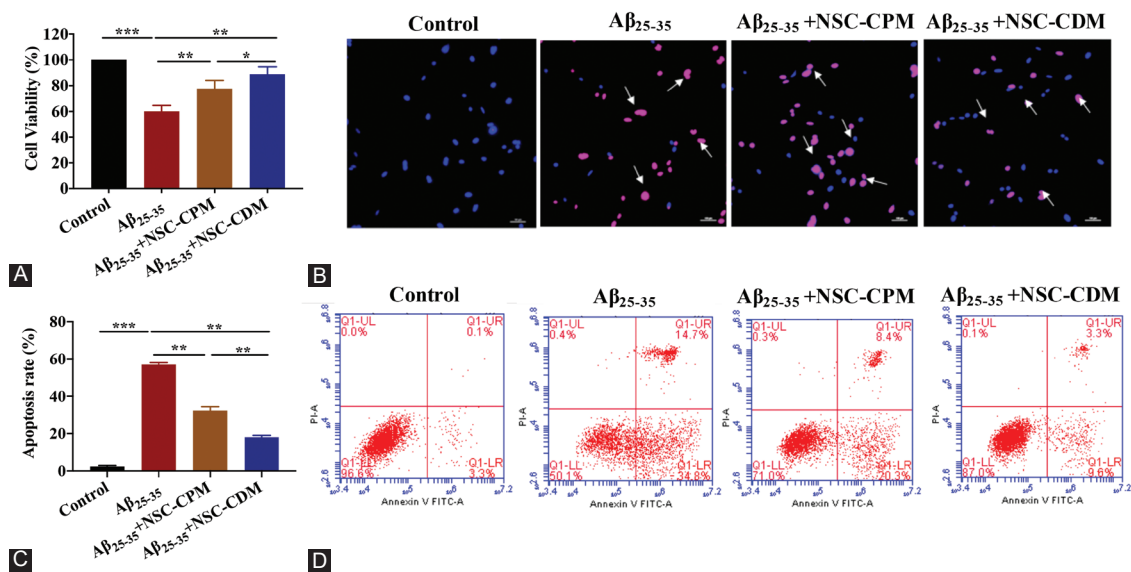


FIGURE 2. Neural stem cell-conditioned medium (NSC-CDM) protected against $A\beta_{25-35}$ -induced toxicity, including decreased cell viability and increased apoptosis, in SH-SY5Y cells. (A) The cell viability of SH-SY5Y cells was evaluated by CCK-8 assay in the control, $A\beta_{25-35}$ (40 μM), $A\beta_{25-35}$ (40 μM) + neural stem cell-complete medium (NSC-CPM), and $A\beta_{25-35}$ (40 μM) + NSC-CDM groups for 24 h. (B and C) The apoptotic rates of the cells were labeled with the TUNEL assay in the control, $A\beta_{25-35}$ (40 μM), $A\beta_{25-35}$ (40 μM) + NSC-CPM, and $A\beta_{25-35}$ (40 μM) + NSC-CDM groups for 24 h. The white arrow represents apoptotic cells. Scale bar = 100 μm . (D) Apoptotic cells were examined by annexin V-FITC/PI double-staining in the control, $A\beta_{25-35}$ (40 μM), $A\beta_{25-35}$ (40 μM) + NSC-CPM, and $A\beta_{25-35}$ (40 μM) + NSC-CDM groups for 24 h. * $p < 0.05$, ** $p < 0.01$, *** $p < 0.001$. $A\beta_{25-35}$ significantly decreased the cell viability of SH-SY5Y cells as compared with the control group. In contrast, both NSC-CPM and NSC-CDM had an inhibitory effect on the cytotoxicity induced by $A\beta_{25-35}$, with the NSC-CDM group demonstrating a higher cell viability than the NSC-CPM group. Next, we applied TUNEL and Annexin V-FITC/PI double-staining to determine the number of apoptotic SH-SY5Y cells. The nuclear fragmentation that is a characteristic feature of apoptotic cells was clearly observed in the $A\beta_{25-35}$ -induced SH-SY5Y cells. In addition, condensed nuclei were also identified. However, the numbers of TUNEL-positive nuclei were significantly lower in the NSC-CPM or NSC-CDM + $A\beta_{25-35}$ -treated cells, with the NSC-CDM group demonstrating a lower number of TUNEL-positive nuclei than the NSC-CPM group. In addition, cellular apoptosis was examined by Annexin V-FITC/PI double-staining and showed the same trends.

NSC-CDM protected against mitochondrial pathway-related apoptosis induced by $A\beta_{25-35}$ in SH-SY5Y cells

To further clarify how NSC-CDM protected against mitochondrial pathway apoptosis induced by $A\beta_{25-35}$, we detected ROS, MDA, MMP, and mitochondrial pathway

apoptosis-related proteins in the control, $A\beta_{25-35}$ (40 μM), $A\beta_{25-35}$ (40 μM) + NSC-CPM, and $A\beta_{25-35}$ (40 μM) + NSC-CDM groups. ROS assays showed that the ROS content of the $A\beta_{25-35}$ group was significantly higher than that of the control group ($p < 0.001$). The ROS contents in the NSC-CPM and NSC-CDM+ $A\beta_{25-35}$ groups were significantly lower than

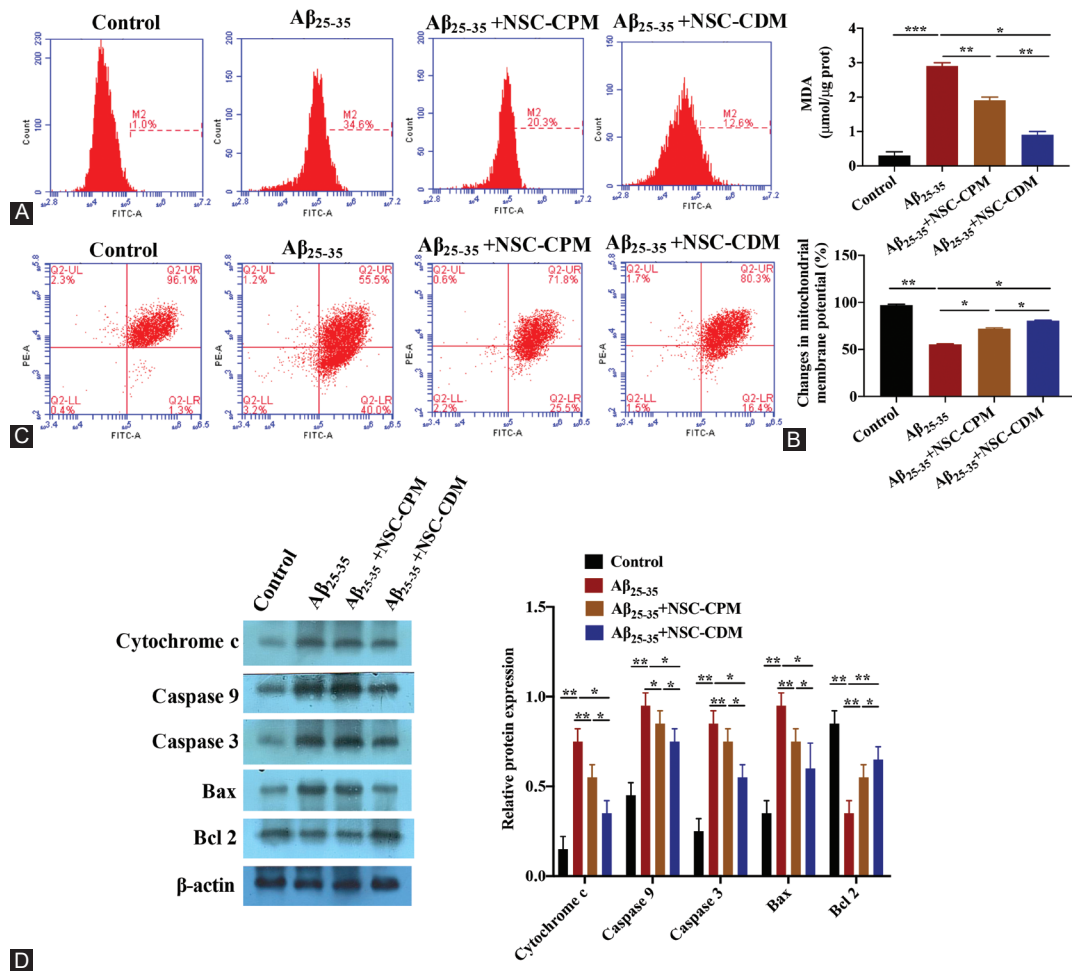


FIGURE 3. Neural stem cell-conditioned medium (NSC-CDM) protected against mitochondrial pathway-related apoptosis in SH-SY5Y cells induced by A β_{25-35} . (A) Flow cytometry was used to detect the relative intensity of reactive oxygen species (ROS) in the SH-SY5Y cells in the control, A β_{25-35} (40 μM), A β_{25-35} (40 μM) + NSC-CPM, and A β_{25-35} (40 μM) + NSC-CDM groups for 24 h. (B) The MDA contents of the SH-SY5Y cells were assessed by ELISA kits in the control, A β_{25-35} (40 μM), A β_{25-35} (40 μM) + NSC-CPM, and A β_{25-35} (40 μM) + NSC-CDM groups for 24 h. (C) Changes in the MMP by JC-1 in the control, A β_{25-35} (40 μM), A β_{25-35} (40 μM) + NSC-CPM, and A β_{25-35} (40 μM) + NSC-CDM groups for 24 h. (D) Cytochrome c, caspase-9, caspase-3, Bcl-2-associated X protein (Bax), and B-cell lymphoma 2 (Bcl-2) protein expressions were evaluated by Western blot analysis in the control, A β_{25-35} (40 μM), A β_{25-35} (40 μM) + NSC-CPM, and A β_{25-35} (40 μM) + NSC-CDM groups for 24 h. * $p < 0.05$, ** $p < 0.01$, *** $p < 0.001$. The ROS content of the A β_{25-35} group was significantly higher than that of the control group. The ROS content in the NSC-CPM and NSC-CDM+A β_{25-35} group was significantly lower than that in the A β_{25-35} group. The results of MDA content assays were similar to those of ROS assays. In addition, a decrease in MMP became obvious in the A β_{25-35} group. These effects were reversed by the administration of NSC-CPM or NSC-CDM. The results from the Western blot analysis showed a decrease in the Bcl-2 expression level and an increase in the cytochrome c, caspase-9, caspase-3, and Bax expression levels in the A β_{25-35} group compared with the control group.

that in the A β_{25-35} group ($p < 0.01$ and $p < 0.05$, respectively; Figure 3A). The results of the MDA content assays were similar to those of the ROS assays (Figure 3B). In addition, a decrease in the MMP became obvious in the A β_{25-35} group. These effects were reversed by the administration of NSC-CPM or NSC-CDM (Figure 3C). To further clarify how NSC-CDM inhibited mitochondrial pathway apoptosis, we used Western blot analysis to measure the expressions of cytochrome c, caspase-9, caspase-3, Bax, and Bcl-2 in the control, A β_{25-35} (40 μM), A β_{25-35} (40 μM) + NSC-CPM, and A β_{25-35} (40 μM) + NSC-CDM groups. As illustrated in Figure 3D, the results from the Western blot analysis showed a decrease in the Bcl-2 expression level and an increase in the cytochrome

c, caspase-9, caspase-3, and Bax expression levels in the A β_{25-35} group compared with the control group (all $p < 0.01$). These effects were further ameliorated by the administration of NSC-CPM or NSC-CDM.

NSC-CDM protected against A β_{25-35} -induced mitochondrial ultrastructure damage in SH-SY5Y cells

To further clarify whether NSC-CDM had the capacity to protect the ultrastructure of the mitochondria, we used TEM to observe mitochondrial morphology in the control, A β_{25-35} (40 μM), A β_{25-35} (40 μM) + NSC-CPM, and A β_{25-35} (40 μM) + NSC-CDM groups. As illustrated in Figure 4, mitochondrial

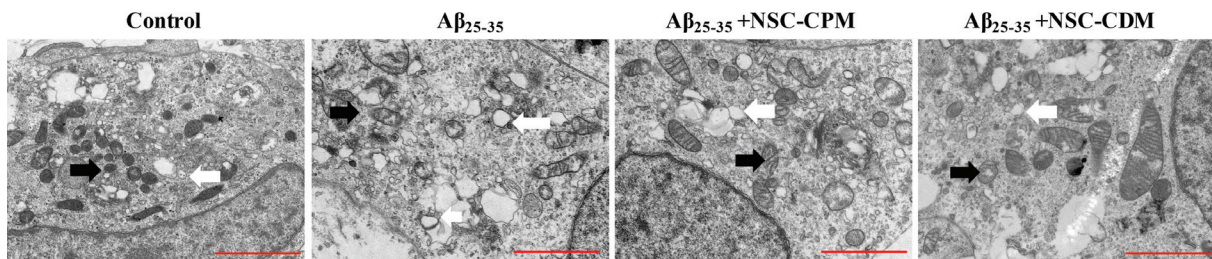


FIGURE 4. Transmission electron microscopy was used to detect the ultrastructure of the mitochondria in the SH-SY5Y cells in the control, A β_{25-35} (40 μ M), A β_{25-35} (40 μ M) + neural stem cell-conditioned medium (NSC-CPM), and A β_{25-35} (40 μ M) + NSC-CDM groups for 24 h. The black arrow indicates normal mitochondria, whereas the white arrow indicates swollen mitochondria. Scale bar = 2 μ m. Mitochondrial swelling was observed in the SH-SY5Y cells treated with A β_{25-35} . In particular, the crista of the mitochondria was observed to almost disappear or disintegrate. However, in the NSC-CPM and NSC-CDM+A β_{25-35} groups, although most of the mitochondria were swollen and disrupted, we observed some normal mitochondria with the crista split. In addition, mitochondrial swelling in the NSC-CDM + A β_{25-35} group was considered mild compared with that of the NSC-CPM + A β_{25-35} group.

swelling was observed in the SH-SY5Y cells treated with A β_{25-35} . In particular, the crista of the mitochondria was observed to almost disappear or disintegrate. However, in the NSC-CPM and NSC-CDM+A β_{25-35} groups, although most of the mitochondria were swollen and disrupted, we observed some normal mitochondria with the crista split. In addition, mitochondrial swelling in the NSC-CDM + A β_{25-35} group was considered mild compared with that of the NSC-CPM + A β_{25-35} group. Therefore, our results indicated the maintenance of the mitochondrial ultrastructure by the administration of NSC-CPM or NSC-CDM.

DISCUSSION

AD is a neurodegenerative disease associated with aging and is considered to be the most common form of dementia. The causes of AD include the accumulation of A β , oxidative stress, inflammation, and a dysfunction in various pathways, including those related to hormones and the mitochondria [13]. In addition, increased proteolytic degradation of amyloid precursor protein (APP) and the aggregation and deposition of A β are considered to be two characteristic pathologies in the development and progression of AD [14]. In particular, A β_{25-35} is a core toxic fragment of the full-length A β peptide [15] that easily penetrates the cell membrane due to its small size. In addition, the toxicity of A β_{25-35} is similar to that of A β_{1-40} and A β_{1-42} [16]. However, A β_{25-35} is a particularly difficult-to-treat peptide because it aggregates rapidly and it quickly becomes toxic, whereas full-length A β needs to age for more than a week to aggregate [17]. Therefore, A β_{25-35} is commonly used in *in vitro* studies to predict the neuroprotective effects of various drugs that modulate A β toxicity [18]. In our current study, A β_{25-35} (40 μ M) decreased the cell viability of SH-SY5Y cells in a time- and concentration-dependent manner.

Previous studies have demonstrated that NSCs can promote the recovery of the nervous system through direct action (i.e.,

neural replacement) [19] and the indirect bystander secretion of brain-derived neurotrophic factor (BDNF) [20], thereby inhibiting the inflammatory process and enhancing internal glial production [21]. However, the original sources and low survival and neuron differentiation rates [22], along with the potential for NSC tumor formation [23], have limited the clinical application of NSCs. Historically, NSC-CDM has always been discarded as waste because NSCs produce potentially harmful substances in the NSC-CDM during cell division *in vitro*. However, in recent years, NSC-CDM has received increasing attention due to the extensive study of the bystander behavior of NSCs *in vivo*, particularly that of the microvesicles released by NSCs. In addition, NSC-CDM has been shown to exert anti-apoptotic effects both *in vitro* [24] and *in vivo* [11]. To circumvent these potential obstacles and find new therapeutic strategies to treat AD, we first explored the effect of NSC-CDM in A β_{25-35} -induced SH-SY5Y cells and we consider that NSC-CDM may be an effective treatment for AD. Indeed, our data showed that A β_{25-35} significantly decreased cell viability and induced apoptosis in the SH-SY5Y cells, whereas NSC-CDM or NSC-CPM had an inhibitory effect on this toxicity when fibrillation of A β_{25-35} occurred. However, an *in vitro* model always has limitations; therefore, animal experiments should be considered in the future.

The oxidation of ROS leads to oxidative damage and neuronal cell death and is known to play an important role in the pathogenesis of neurodegenerative diseases. Antioxidants have been proposed to prevent the toxicity caused by A β_{25-35} in AD [25]. Previous studies have shown that MDA inhibits mitochondrial complex I- and complex II-linked respiration and reduces MMP, leading to mitochondrial dysfunction [26]. Bax, a homologous protein to Bcl-2, is a pro-apoptotic protein, while Bcl-2 is an anti-apoptotic protein that inhibits apoptosis. Therefore, the respective levels of Bax and Bcl-2 are considered to be directly related to the regulation of apoptosis. In addition, cytochrome c is an essential component of the respiratory chain and plays an important role in redox and energy

metabolism, while also being a key component of the mitochondrial initiation of apoptosis [27]. In this process, the Bax protein acts as a component of the ion channel on the mitochondrial membrane and the upregulation of Bax allows for cytochrome c to cross the mitochondrial membrane, thereby activating the initiation of apoptosis through the activation of caspase-9. Further activation of caspase-3 in the apoptotic cascade results in cellular apoptosis [28]. The downregulation of Bcl-2 prevents it from interfering with cytochrome c release, thereby activating the caspase protease activity of upstream apoptotic proteins and promoting cellular apoptosis [29]. In the present study, the ROS contents of the NSC-CDM and NSC-CPM groups were significantly decreased in A β_{25-35} -induced SH-SY5Y cells. The results of MDA content assays were similar to those of ROS production assays. In addition, the associated decrease in the MMP was reversed by treatment with NSC-CDM or NSC-CPM. Furthermore, the Western blot results showed that the decreased Bcl-2 expression level and the increased expression levels of cytochrome c, caspase-9, caspase-3, and Bax induced by A β_{25-35} were ameliorated by NSC-CDM or NSC-CPM.

Autophagy is an important mechanism for self-protection and self-renewal of cells [30]. Oxidative stress leads to the degradation of mitochondria and the generation of abnormal proteins that cannot be degraded by the ubiquitin-proteasome system, thus requiring autophagy [31]. Indeed, the timely degradation of excess, damaged, and aging proteins and organelles prevents oxidative stress cascades, while also providing essential materials for cellular reconstitution, regeneration and repair, thus maintaining cellular homeostasis. Collectively, our findings indicated that A β_{25-35} induced damage to the mitochondrial ultrastructure, which was reversed by NSC-CDM or NSC-CPM treatment.

CONCLUSION

This study demonstrated the protective effect of NSC-CDM on A β_{25-35} -induced damage in SH-SY5Y cells and clarified the mechanism of action of A β_{25-35} in terms of mitochondrial function maintenance and mitochondria-associated apoptosis signaling pathways, thus providing a theoretical basis for the development of novel anti-AD treatments.

REFERENCES

- [1] Shah H, Albanese E, Duggan C, Rudan I, Langa KM, Carrillo MC, et al. Research priorities to reduce the global burden of dementia by 2025. *Lancet Neurol* 2016;15(12):1285-94. [https://doi.org/10.1016/S1474-4422\(16\)30235-6](https://doi.org/10.1016/S1474-4422(16)30235-6).
- [2] Forner S, Baglietto-Vargas D, Martini AC, Trujillo-Estrada L, LaFerla FM. Synaptic impairment in Alzheimer's disease: A dysregulated symphony. *Trends Neurosci* 2017;40(6):347-57. <https://doi.org/10.1016/j.tins.2017.04.002>.
- [3] Leuner K, Müller WE, Reichert AS. From mitochondrial dysfunction to amyloid beta formation: Novel insights into the pathogenesis of Alzheimer's disease. *Mol Neurobiol* 2012;46(1):186-93. <https://doi.org/10.1007/s12035-012-8307-4>.
- [4] Rubio-Moscardo F, Setó-Salvia N, Pera M, Bosch-Morató M, Plata C, Belbin O, et al. Rare variants in calcium homeostasis modulator 1 (CALHM1) found in early onset Alzheimer's disease patients alter calcium homeostasis. *PLoS One* 2013;8(9):e74203. <https://doi.org/10.1371/journal.pone.0074203>.
- [5] Landgren H, Curtis MA. Locating and labeling neural stem cells in the brain. *J Cell Physiol* 2011;226(1):1-7. <https://doi.org/10.1002/jcp.22319>.
- [6] Lewis S. Neurodegenerative disease: Remodelling neurodegeneration. *Nat Rev Neurosci* 2018;19(1):3. <https://doi.org/10.1038/nrn.2017.152>.
- [7] Hwang DH, Shin HY, Kwon MJ, Choi JY, Ryu BY, Kim BG. Survival of neural stem cell grafts in the lesioned spinal cord is enhanced by a combination of treadmill locomotor training via insulin-like growth factor-1 signaling. *J Neurosci* 2014;34(38):12788-800. <https://doi.org/10.1523/jneurosci.5359-13.2014>.
- [8] Yousefifard M, Rahimi-Movaghar V, Nasirinezhad F, Baikpour M, Safari S, Saadat S, et al. Neural stem/progenitor cell transplantation for spinal cord injury treatment; A systematic review and meta-analysis. *Neuroscience* 2016;322:377-97. <https://doi.org/10.1016/j.neuroscience.2016.02.034>.
- [9] Dooley D, Vidal P, Hendrix S. Immunopharmacological intervention for successful neural stem cell therapy: New perspectives in CNS neurogenesis and repair. *Pharmacol Ther* 2014;141(1):21-31. <https://doi.org/10.1016/j.pharmthera.2013.08.001>.
- [10] Cheng Z, Bosco DB, Sun L, Chen X, Xu Y, Tai W, et al. Neural stem cell-conditioned medium suppresses inflammation and promotes spinal cord injury recovery. *Cell Transplant* 2017;26(3):469-82. <https://doi.org/10.3727/096368916x693473>.
- [11] Liang P, Liu J, Xiong J, Liu Q, Zhao J, Liang H, et al. Neural stem cell-conditioned medium protects neurons and promotes propriospinal neurons relay neural circuit reconnection after spinal cord injury. *Cell Transplant* 2014;23 Suppl 1:S45-56. <https://doi.org/10.3727/096368914x684989>.
- [12] Yang H, Wang C, Chen H, Li L, Ma S, Wang H, et al. Neural stem cell-conditioned medium ameliorated cerebral ischemia-reperfusion injury in rats. *Stem Cells Int* 2018;2018:4659159. <https://doi.org/10.1155/2018/4659159>.
- [13] Doraiswamy PM. Non-cholinergic strategies for treating and preventing Alzheimer's disease. *CNS Drugs* 2002;16(12):811-24. <https://doi.org/10.2165/00023210-200216120-00003>.
- [14] Tsunekawa H, Noda Y, Mouri A, Yoneda F, Nabeshima T. Synergistic effects of selegiline and donepezil on cognitive impairment induced by amyloid beta (25-35). *Behav Brain Res* 2008;190(2):224-32. <https://doi.org/10.1016/j.bbr.2008.03.002>.
- [15] Yang R, Wei L, Fu QQ, You H, Yu HR. SOD3 ameliorates A β_{25-35} -induced oxidative damage in SH-SY5Y cells by inhibiting the mitochondrial pathway. *Cell Mol Neurobiol* 2017;37(3):513-25. <https://doi.org/10.1007/s10071-016-0390-z>.
- [16] Mark RJ, Keller JN, Kruman I, Mattson MP. Abeta25-35 induces rapid lysis of red blood cells: Contrast with Abeta1-42 and examination of underlying mechanisms. *Brain Res* 1997;756(1):205-14. [https://doi.org/10.1016/S0006-8993\(97\)00824-X](https://doi.org/10.1016/S0006-8993(97)00824-X).
- [17] Hughes E, Burke RM, Doig AJ. Inhibition of toxicity in the beta-amyloid peptide fragment beta (25-35) using N-methylated derivatives: A general strategy to prevent amyloid formation. *J Biol Chem* 2000;275(33):25109-15. <https://doi.org/10.1074/jbc.m003554200>.
- [18] Yu H, Yao L, Zhou H, Qu S, Zeng X, Zhou D, et al. Neuroprotection against A β_{25-35} -induced apoptosis by *Salvia miltiorrhiza* extract in SH-SY5Y cells. *Neurochem Int* 2014;75:89-95. <https://doi.org/10.1016/j.neuint.2014.06.001>.
- [19] Cheng Y, Zhang J, Deng L, Johnson NR, Yu X, Zhang N, et al. Intravenously delivered neural stem cells migrate into ischemic brain, differentiate and improve functional recovery after transient ischemic stroke in adult rats. *Int J Clin Exp Pathol* 2015;8(3):2928-36.
- [20] Ratajczak MZ, Kucia M, Jadczyk T, Greco NJ, Wojakowski W, Tendera M, et al. Pivotal role of paracrine effects in stem cell

- therapies in regenerative medicine: Can we translate stem cell-secreted paracrine factors and microvesicles into better therapeutic strategies? *Leukemia* 2012;26(6):1166-73.
<https://doi.org/10.1038/leu.2011.389>.
- [21] Ryu S, Lee SH, Kim SU, Yoon BW. Human neural stem cells promote proliferation of endogenous neural stem cells and enhance angiogenesis in ischemic rat brain. *Neural Regen Res* 2016;11(2):298-304.
<https://doi.org/10.4103/1673-5374.177739>.
- [22] Tang YH, Ma YY, Zhang ZJ, Wang YT, Yang GY. Opportunities and challenges: Stem cell-based therapy for the treatment of ischemic stroke. *CNS Neurosci Ther* 2015;21(4):337-47.
<https://doi.org/10.1111/cns.12386>.
- [23] Doepfner TR, Hermann DM. Stem cell-based treatments against stroke: Observations from human proof-of-concept studies and considerations regarding clinical applicability. *Front Cell Neurosci* 2014;8:357.
<https://doi.org/10.3389/fncel.2014.00357>.
- [24] Yang H, Wang J, Sun J, Liu X, Duan WM, Qu T. A new method to effectively and rapidly generate neurons from SH-SY5Y cells. *Neurosci Lett* 2016;610:43-7.
<https://doi.org/10.1016/j.neulet.2015.10.047>.
- [25] Jung Choi S, Kim MJ, Jin Heo H, Kim JK, Jin Jun W, Kim HK, et al. Ameliorative effect of 1,2-benzenedicarboxylic acid dinonyl ester against amyloid beta peptide-induced neurotoxicity. *Amyloid* 2009;16(1):15-24.
<https://doi.org/10.1080/13506120802676997>.
- [26] Zhang WP, Zong QF, Gao Q, Yu Y, Gu XY, Wang Y, et al. Effects of endomorphin-1 postconditioning on myocardial ischemia/reperfusion injury and myocardial cell apoptosis in a rat model. *Mol Med Rep* 2016;14(4):3992-8.
<https://doi.org/10.3892/mmr.2016.5695>.
- [27] Williams CH Jr., Kamin H. Microsomal triphosphopyridine nucleotide-cytochrome c reductase of liver. *J Biol Chem* 1962;237:587-95.
- [28] Schon EA, Manfredi G. Neuronal degeneration and mitochondrial dysfunction. *J Clin Invest* 2003;111(3):303-12.
<https://doi.org/10.1172/jci200317741>.
- [29] Voutsadakis IA. Apoptosis and the pathogenesis of lymphoma. *Acta Oncol* 2000;39(2):151-6.
<https://doi.org/10.1080/028418600430707>.
- [30] Coto-Montes A, Boga JA, Rosales-Corral S, Fuentes-Broto L, Tan DX, Reiter RJ. Role of melatonin in the regulation of autophagy and mitophagy: A review. *Mol Cell Endocrinol* 2012;361(1-2):12-23.
<https://doi.org/10.1016/j.mce.2012.04.009>.
- [31] Lynch-Day MA, Mao K, Wang K, Zhao M, Klionsky DJ. The role of autophagy in Parkinson's disease. *Cold Spring Harb Perspect Med* 2012;2(4):a009357.
<https://doi.org/10.1101/cshperspect.a009357>.

Related articles published in BJBMS

1. [Asymptomatic neurotoxicity of amyloid \$\beta\$ -peptides \(A \$\beta\$ 1-42 and A \$\beta\$ 25-35\) on mouse embryonic stem cell-derived neural cells](#)
 Nur Izzati Mansor et al., BJBMS, 2020
2. [The neuroprotective effects of tocotrienol rich fraction and alpha tocopherol against glutamate injury in astrocytes](#)
 Thilaga Rati Selvaraju et al., BJBMS, 2014